Available online at www.sciencedirect.com

SciVerse ScienceDirect

Procedia IUTAM 00 (2013) 000–000

Procedia IUTAM

www.elsevier.com/locate/procedia

Nonlinear Interfacial Wave Phenomena from the Micro- to the Macro-Scale

Computation of three-dimensional flexural-gravity solitary waves in arbitrary depth

Zhan Wang[a], Paul A. Milewski[b,*], Jean-Marc Vanden-Broeck[a]

[a]*Department of Mathematics, University College London, Gower Street, London, WC1E 6BT, UK.*
[b]*Department of Mathematical Sciences, University of Bath, Bath, BA2 7AY, UK.*

Abstract

Fully-localised solitary waves propagating on the surface of a three-dimensional ideal fluid of arbitrary depth, and bounded above by an elastic sheet that resists flexing, are computed. The cases of shallow and deep water are distinct. In shallow water, weakly nonlinear modulational analysis (see Milewski & Wang[6]) predicts waves of arbitrarily small amplitude and these are found numerically. In deep water, the same analysis rules out the existence of solitary waves bifurcating from linear waves, but, nevertheless, we find them at finite amplitude. This is accomplished using a continuation method following the branch from the shallow regime. All solutions are computed via a fifth-order Hamiltonian truncation of the full ideal free-boundary fluid equations. We show that this truncation is quantitatively accurate by comparisons with full potential flow in two-dimensions.

Keywords: Solitary Waves, Water Waves, Flexural-Gravity Waves

1. Introduction

Fully localised travelling disturbances of a flexible sheet on the surface of a fluid, often called the flexural-gravity (FG) wave problem, are considered. This problem has been proposed as a model for the dynamics of waves under floating ice sheet, and has, mostly in the linear setting, been studied extensively (the reader is referred to the monograph by Squire *et al.*[13] and the references therein). The main application of these studies has been the use of lake and ocean ice for roadways and landing strips or for the understanding of how disturbances arising from water waves impinging on the edge of an ice sheet propagate. Another possible offshoot of this research is the dynamics of man-made floating structures which have been studied in the past in the context of floating bridges' and airports' structural integrity. There is renewed interest in understanding ice sheet dynamics and its breakup due to many effects, including waves, as it has an important impact on the climate.

Recent nonlinear studies have aimed to understand the large response of ice to moving forces when the forces move at particular (constant) speeds. These studies have been restricted to the one-dimensional free surface of a

* Corresponding author. Tel.: +44 (0) 1225 386224.
E-mail address: p.a.milewski@bath.ac.uk

two-dimensional fluid (the 2D problem). Milewski *et al.*[5] found that forces moving at a critical range of speeds could generate a strongly nonlinear, large-amplitude and stable localized response. This phenomenon was also computed by Guyenne & Părău[3,4] using a different fully nonlinear elastic model. As pointed out in these papers, in order to understand these forced responses it is crucial to know the nontrivial free responses of the system, such as fully localised solitary waves.

Three-dimensional (3D) nonlinear FG waves have not been studied extensively, the first challenge being finding appropriate models for the solid. In the simplest nonlinear shell theories of fully nonlinear elasticity Plotnikov & Toland[12] posed an energy due to the bending only (i.e. beam-like response) of the thin material using the Willmore functional. Milewski & Wang[6] used this model to investigate the problem in the weakly nonlinear modulational regime which resulted in the Benney-Roskes-Davey-Stewartson (BRDS) system whose type varies with the physical parameters of the problem. They found that at the minimum of phase speed, which is the regime at which localised travelling wave solutions bifurcate, the BRDS system was defocussing (Benjamin-Feir stable) in infinite depth and focussing for water shallower than a critical depth. Thus in the infinite depth limit one does not expect small amplitude localised solutions whereas in water shallower than the critical depth the physics sustains bright solitary waves of BRDS corresponding to small-amplitude wave packet solitary waves in the original problem. In the two-dimensional FG problem, however, fully localised travelling wave solutions were found in infinite depth (Guyenne & Părău[3], Milewski *et al.*[5]), even though the associated nonlinear Schrödinger equation (NLS) which is the counterpart of BRDS for the 2D problem is also of defocussing type. These solutions do not exist at arbitrarily small amplitude, and bifurcate from *finite amplitude* generalised solitary waves. The question remains whether similar results hold in 3D (especially the existence of finite amplitude waves in infinite depth), and we address it in this paper. In Părău & Vanden-Broeck[10] one example of an unforced solution with a *linear* elasticity model is shown, but more computations are needed to understand the properties of solitary waves for this model.

In addition to the challenge mentioned above regarding the model for the solid, the 3D problem has the added difficulty of the lack of accurate and efficient 3D numerical formulations for the fluid. Boundary integral methods have been used both in this problem with linear elasticity and the similar capillary-gravity problem (Părău & Vanden-Broeck[9,10], Părău *et al.*[11]) but it is computationally expensive to obtain highly accurate results (see, for example, Wang & Milewski[15]). Here, we numerically compute 3D FG solitary waves via a quintic truncation Hamiltonian model both in shallow and deep water. The model is first validated against full potential flow calculations in 2D. We then show, numerically, that there exist fully localised FG travelling waves for all values of depth in 3D, and that in shallow water these waves exist at arbitrary small amplitudes (as predicted by BRDS) whereas in deep water and in infinite depth, the waves exist only at finite amplitude. To our knowledge, these are the first computations of solution branches for 3D localised flexural-gravity waves for the Plotnikov & Toland's model.

The rest of the paper is structured as follows: in Section 2, we formulate the FG problem mathematically; in Section 3, we briefly present the derivation of different truncated models and discuss what can be learned about the solitary waves from the associated BRDS system; in Section 4, we validate models by investigating comparisons between different models and the full problem in 2D. This is followed by the main numerical results of the existence of solitary waves, especially in a deep water situation, when the associated BRDS system is of the defocussing type. Lastly, some concluding remarks are presented in Section 5.

2. Formulation

2.1. Mathematical Description

Consider an incompressible, inviscid, irrotational, three dimensional fluid covered by an elastic sheet on the top and a rigid horizontal wall at the bottom. The restoring forces are due to gravity and the elastic bending. The Hamiltonian of the problem is the total energy of the fluid which is the sum of kinetic and potential energies (Zakharov[18]):

$$\begin{aligned}\mathcal{H}[\eta,\xi] &= \frac{1}{2}\int dxdy\int_{-H_0}^{\eta}\left(\phi_x^2+\phi_y^2+\phi_z^2\right)dz+\frac{1}{2}\int\eta^2dxdy+\frac{1}{2}\int(\kappa_1+\kappa_2)^2dS\\ &= \frac{1}{2}\int\xi G(\eta)\xi dxdy+\frac{1}{2}\int\eta^2dxdy+\frac{1}{2}\int(\kappa_1+\kappa_2)^2dS\end{aligned}\tag{1}$$

where $\phi(x,y,z,t)$ is the velocity potential whose gradient is the velocity field of the fluid, $\eta(x,y,t)$ is the free surface displacement, H_0 is the mean depth of the fluid, $\xi = \phi(x,y,\eta(x,y,t),t)$ is designated as the surface potential, κ_1 and κ_2 are the principal curvatures on the free surface, and dS is the surface element. $G(\eta)$ is a scaled Dirichlet to Neumann (DtN) operator yielding the normal velocity of the free surface. It is defined by $G(\eta) \triangleq \phi_z - \nabla\phi\cdot\nabla\eta = \sqrt{1+|\nabla\eta|^2}\,\phi_{\mathbf{n}}$, where $\phi_{\mathbf{n}}$ is the derivative of the potential in the outward normal direction to the free surface. The Willmore surface energy in (1) was proposed by Plotnikov & Toland[12] for this problem and later written in the Euler-Lagrangian form by Milewski & Wang[6] to study the wavepacket FG solitary waves in the modulational regime. We note that the total energy (1) is in non-dimensional form, with the density of the fluid, the gravitational acceleration and the flexural rigidity of the surface solid, having been removed by proper rescaling. The only parameter remaining is the mean depth which appears in G (see below).

Following Zakharov[18], who worked in these canonical variables, the kinematic and dynamic boundary conditions can be recast in terms of ξ and η as:

$$\eta_t = \frac{\delta\mathcal{H}}{\delta\xi} = G(\eta)\xi \tag{2}$$

$$\xi_t = -\frac{\delta\mathcal{H}}{\delta\eta} = \frac{1}{2J}\Big[(G(\eta)\xi)^2 + 2(G(\eta)\xi)(\nabla\xi\cdot\nabla\eta) - \big|\nabla\xi\big|^2\big|\nabla\eta\big|^2 + (\nabla\xi\cdot\nabla\eta)^2 - \big|\nabla\xi\big|^2\Big] - \eta - \frac{\delta E_b}{\delta\eta} \tag{3}$$

where $E_b \triangleq \frac{1}{2}\int(\kappa_1+\kappa_2)^2 dS$, and its variational derivative takes the form:

$$\begin{aligned}\frac{\delta E_b}{\delta\eta} = &-2\partial_x\Big[\kappa\,\frac{\eta_x\eta_{yy}-\eta_y\eta_{xy}}{J}\Big] - 2\partial_y\Big[\kappa\,\frac{\eta_y\eta_{xx}-\eta_x\eta_{xy}}{J}\Big] - 2\partial_{xy}\Big[\kappa\,\frac{\eta_x\eta_y}{J}\Big]\\ &+\partial_{xx}\Big[\kappa\,\frac{1+\eta_y^2}{J}\Big] + \partial_{yy}\Big[\kappa\frac{1+\eta_x^2}{J}\Big] + \frac{5}{2}\partial_x\Big[\kappa^2\frac{\eta_x}{\sqrt{J}}\Big] + \frac{5}{2}\partial_y\Big[\kappa^2\frac{\eta_y}{\sqrt{J}}\Big]\end{aligned} \tag{4}$$

where

$$J = 1+\eta_x^2+\eta_y^2 \tag{5}$$

$$\kappa = \kappa_1+\kappa_2 = \frac{(1+\eta_x^2)\eta_{yy} + (1+\eta_y^2)\eta_{xx} - 2\eta_x\eta_y\eta_{xy}}{J^{3/2}} \tag{6}$$

2.2. Dirichelet to Neumann Expansion

The key difficulty in solving the surface water wave problem (2–3) using this formulation is how to compute the DtN operator. It has been proved under quite general conditions that the DtN operator $G(\eta)$ is analytic therefore can be expanded as a convergent Taylor series $G = \sum_{i=0}^{\infty} G_i$. Craig & Sulem[2] first showed the explicit expression for G_i using a recursion formula. The readers can find the derivation of the formula in Craig & Sulem[2] and the references therein. The recursive representation was then rewritten (see Craig & Nicholls[1], Nicholls & Reitich[7], Xu & Guyenne[17]) using the adjoint operator of G, which is much simpler to use numerically. Using the adjoint formula, the resulting recursion form for the DtN operator is given as follows: for $j = 2r > 0$,

$$\begin{aligned}G_{2r}(\eta) = &\frac{1}{(2r)!}\,G_0(|D|^2)^{r-1}D\cdot\eta^{2r}D - \sum_{s=0}^{r-1}\frac{1}{(2(r-s))!}(|D|^2)^{r-s}\eta^{2(r-s)}G_{2s}(\eta)\\ &-\sum_{s=0}^{r-1}\frac{1}{(2(r-s)-1)!}G_0(|D|^2)^{r-s-1}\eta^{2(r-s)-1}G_{2s+1}(\eta),\end{aligned} \tag{7}$$

and, for $j = 2r-1 > 0$,

$$\begin{aligned}G_{2r-1}(\eta) = &\frac{1}{(2r-1)!}\,(|D|^2)^{r-1}D\cdot\eta^{2r-1}D - \sum_{s=0}^{r-1}\frac{1}{(2(r-s)-1)!}G_0(|D|^2)^{r-s-1}\eta^{2(r-s)-1}G_{2s}(\eta)\\ &-\sum_{s=0}^{r-2}\frac{1}{(2(r-s-1))!}(|D|^2)^{r-s-1}\eta^{2(r-s-1)}G_{2s+1}(\eta),\end{aligned} \tag{8}$$

with

$$G_0 = |D| \tanh\left(H_0|D|\right) \tag{9}$$

where $D = -i\nabla$ and $|D|^2 = -\Delta$. It is noted that as $H_0 \to \infty$, G_0 reduces to $|D|$. Computation of the DtN operator via the adjoint formulae (7) and (8) is substantially faster and memory efficient than the original formulae presented in Craig & Sulem [2].

3. Approximate Equations

3.1. Truncation and Models

There are three main ways in which the water wave problem can be approximated. First, one can truncate the DtN expansion in the Hamiltonian (1), take the variational derivatives to obtain dynamical equations, and then evolve these equations (this will be called the Hamiltonian expansion method and was used in Wang & Milewski [15]). Second, one can take the exact evolution equations (2–3) and substitute an DtN expansion of arbitrary order (this will be called the DtN expansion method and is used in most other computational papers using the DtN map). These two approximations are *not* the same in equation (3). The former has the advantage that the resulting approximate dynamical system is Hamiltonian, whereas in the later one gains "for free" a *presumably* better approximation to (3) since some higher order terms are included. A third possibility, which is a priori distinct, is to introduce the DtN expansion of G into (2–3) directly (as in the DtN expansion method) and to then 're-truncate' (3) up to $i+2$ order $\eta^i\xi^2$. This method is, at least up to fifth order ($0 \le i \le 3$), provably equivalent to the first method of truncating the Hamiltonian described above. We omit the tedious explicit computation of this equivalence here.

Listed below are the quadratic, cubic, quartic and quintic models using the Hamiltonian expansion method: for the n-th order truncation ($2 \le n \le 5$),

$$\eta_t = \sum_{j=0}^{n-1} G_j\xi \tag{10}$$

$$\xi_t = \sum_{j=2}^{n} \mathcal{N}_j - \eta - \frac{\delta E_b}{\delta \eta} \tag{11}$$

where

$$\mathcal{N}_2 = \frac{1}{2}\Big[(G_0\xi)^2 - \left|\nabla\xi\right|^2\Big] \tag{12}$$

$$\mathcal{N}_3 = \frac{1}{2}\Big[2(G_0\xi)(G_1\xi) + 2(G_0\xi)(\nabla\xi\cdot\nabla\eta)\Big] \tag{13}$$

$$\mathcal{N}_4 = \frac{1}{2}\Big[2(G_0\xi)(G_2\xi) + (G_1\xi)^2 + 2(G_1\xi)(\nabla\xi\cdot\nabla\eta) + (\nabla\xi\cdot\nabla\eta)^2 - \left|\nabla\eta\right|^2(G_0\xi)^2\Big] \tag{14}$$

$$\mathcal{N}_5 = \frac{1}{2}\Big[2(G_0\xi)(G_3\xi) + 2(G_1\xi)(G_2\xi) + 2(G_2\xi)(\nabla\xi\cdot\nabla\eta) - 2\left|\nabla\eta\right|^2(G_0\xi)(G_1\xi) - 2\left|\nabla\eta\right|^2(G_0\xi)(\nabla\xi\cdot\nabla\eta)\Big] \tag{15}$$

Therefore, one obtains four model systems depending of the order $n = 2, 3, 4, 5$ of truncation. These formulations and approximations have reduced the 3D nonlinear water wave problem to a 2D one involving only the variables on the surface, bypassing the solution of the Laplace equation in an irregular domain at every time step. In periodic domains the operators above can be computed efficiently using Fourier methods.

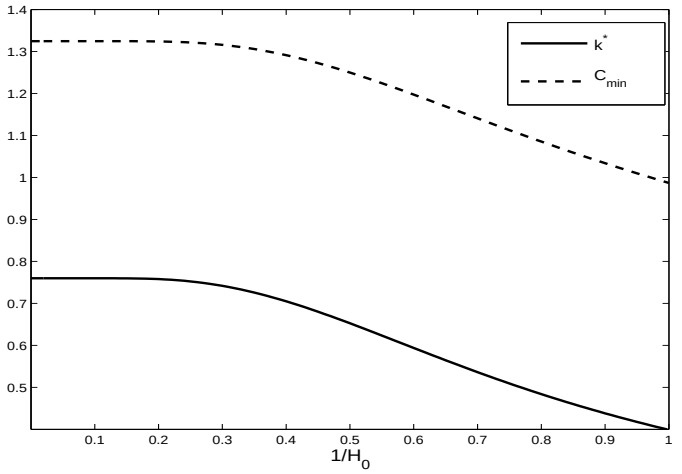

Fig. 1. Plot of the minimum phase speed (dashed line) and corresponding wavenumber (solid line) as the function of the reciprocal of the mean fluid depth $(1/H_0)$.

3.2. Weakly Nonlinear Analysis

All truncation models share the same linear part, and the dispersion relation can be found from the linearized equation:

$$\begin{cases} \eta_t = G_0\xi \\ \xi_t = -\eta - \Delta^2\eta \end{cases} \Longrightarrow \omega^2 = \tanh(|\mathbf{k}|H_0)|\mathbf{k}|(1+|\mathbf{k}|^4) \tag{16}$$

where ω is the frequency and $\mathbf{k} = (k, l)$ is the wavenumber whose components are the wavenumbers in x- and y-direction respectively. The phase speed $c_p(|\mathbf{k}|) \triangleq \frac{\omega(|\mathbf{k}|)}{|\mathbf{k}|}$ has a global minimum $c_{min}(H_0)$ for each fixed H_0. This minimum occurs at wavenumber $|\mathbf{k}| = k^*(H_0)$ and, at this value of $|\mathbf{k}|$, the phase and group speed are equal: $c_g(|\mathbf{k}|) \triangleq \frac{d\omega}{d|\mathbf{k}|} = c_{min}$. These facts imply that steadily travelling wavepacket-like solitary waves may bifurcate from infinitesimal periodic waves of wavenumber k^*, and exist for speed $c < c_{min}$. The bifurcation can be verified by a normal form analysis which is equivalent to deriving the BRDS modulational equations as sketched below. The graphs of k^* and c_{min} are shown in figure 1. In these we can see that, from a linear perspective, $H_0 > 5$ is effectively the infinite depth regime which is expected since $k^*H_0 > 4$.

The results of the BRDS based analysis are briefly stated here, and the reader can find the details for the FG case in Milewski & Wang[6] or Sulem & Sulem[14] for general properties of the system. Just below the global minimum of the phase speed, the quasi-monochromatic waves have the form of small-amplitude wavepackets with crests moving at the same speed as their envelopes. To derive the governing equation for the envelope, we introduce $X = \epsilon(x - c_g t)$, $Y = \epsilon y$ and $T = \epsilon^2 t$, and choose the carrier wave with wavenumber $\mathbf{k} = (k, 0)$ that propagates in x-direction only. One then seeks a solution of the form:

$$\begin{cases} \eta = \epsilon A(X,Y,T)e^{i\Theta} + \epsilon^2 A_1 + \epsilon^3 A_2 + \cdots + \text{c.c.} \\ \phi = \epsilon\Big[\varphi(X,Y,T) + B(X,Y,z,T)e^{i\Theta}\Big] + \epsilon^2 B_1 + \epsilon^3 B_2 + \cdots + \text{c.c.} \end{cases} \tag{17}$$

where $\Theta = kx - \omega t$ and c.c. represents the complex conjugate. A_1, A_2 and B_1, B_2 are higher order corrections that include all the harmonics of the primary mode. Substituting the ansatz (17) into the system (2–3) with the $n = 3$ truncation (higher order terms with $n > 3$ do not enter in the derivation of BRDS) results in the following nonlocal equation equivalent to the BRDS system:

$$iA_T + \frac{\omega''}{2}A_{XX} + \frac{c_g}{2k}A_{YY} + \alpha(k,H_0)\widetilde{\Delta}^{-1}\Big[|A|^2\Big]_{YY}A + \mu(k,H_0)|A|^2A = 0 \tag{18}$$

where $\widetilde{\Delta} = (1 - H_0^{-1}c_g^2)\partial_{XX} + \partial_{YY}$, and all the coefficients ω, c_g, α, μ depend on the wavenumber and the mean depth of the fluid. In Milewski & Wang[6], the authors found that, fixing the wavenumber at $k = k^*(H_0)$ corresponding to the minimum of phase speed described above, the coefficients of dispersion $\omega''/2$ and geometric focussing $c_g/2k$ are both positive, that $\widetilde{\Delta}$ is elliptic, and that there is a critical depth $H_c \approx 233$ such that the controlling nonlinear coefficient $\mu(H_0)$ changes sign, with $\mu < 0$ for $H_0 > H_c$. This fact disallows solitary waves from bifurcating from infinitesimal waves for deeper water ($H_0 > H_c$), and predicts small amplitude localised waves in shallower water ($H_0 < H_c$) arising from fully localised solutions of BRDS (see Milewski & Wang[6]). In next section we shall confirm this numerically in the more primitive Hamiltonian truncation model and show that that solitary waves *also occur* in deeper water at finite amplitude. The FG solitary wave of deep water is a more strongly nonlinear structure, and is not described by the cubic BRDS based analysis.

4. Numerical Results

4.1. Model Validation

In this section we seek fully localised travelling waves translating with speed c to the system (10–11). First of all, we shall determine the required order of truncation in the DtN expansion by comparing the bifurcation curves for different truncated models and for the full irrotational Euler equation in 2D case. In this case the full Euler system can be solved accurately by using a conformal mapping technique Milewski *et al.*[5]. For simplicity in this validation study, we only consider the 2D depression FG solitary waves. In figure 2, we show the speed-amplitude diagrams for $H_0 = 1$, $H_0 = 2$, $H_0 = 5$ and $H_0 = \infty$ for $n = 2, 3, 4, 5$ truncations.

From figure 2 we can see that, if the mean depth of the fluid is small, all the truncation models agree well with the bifurcation picture obtained using the full potential flow equations up to large amplitudes comparable to water depth. However, as H_0 increases, lower order truncations lose accuracy even near c_{min}, and only the quintic model can quantitatively capture the bifurcation diagram for the full potential flow, when $H_0 = \infty$. These observations are intuitively easy to explain. In shallower water the leading nonlinear contribution for water waves is a quadratic term arising from the convective derivatives - thus the quadratic model captures most of the behaviour. As the depth tends to infinity, the cubic truncation *cannot* capture accurately the *finite amplitude* solitary waves (note that the waves computed from the full equations no longer bifurcate from zero amplitude) since, from the BRDS analysis, we know the phenomenon requires omitted higher order terms. The quintic model, however, appears sufficient. The adequacy of the quintic model arises from the observation that for $H_0 > 233$, the nonlinear coefficient μ in the BRDS equation remains very small (see Milewski & Wang[6]) and that, therefore, under a new rescaling, the modulations of wavepackets should be well described by a *cubic-quintic* BRDS model. Furthermore, in order to derive a correct cubic-quintic BRDS equation, the quintic truncation of the DtN expansion is clearly necessary. Although the derivation of a cubic-quintic BRDS equation is tedious and beyond the scope of this work, we conjecture that it would have solitary waves arising from a finite amplitude bifurcation.

Therefore, we conclude that the quintic truncation model is the simplest quantitative DtN-truncated model for FG waves in relatively deep fluids, and that a cubic model is sufficiently accurate in shallower water (certainly for $H_0 < 2$). In the next section we shall use the quintic truncation model in 3D computations for $H_0 \geq 2$ and the cubic model for $H_0 = 1$.

One additional observation can be made from our 2D computations: while the weakly nonlinear analysis predicts that the transition between shallow and deep water behaviour happens at $H_0 \approx 233$, we find that in practice, it occurs in much shallower water. For depths $5 < H_0 < 233$, the controlling nonlinear coefficient μ, whilst positive, remains very small (see Milewski & Wang[6]) and thus the bifurcation curve is predicted to be extremely steep at c_{min}. Numerically, for any speed appreciably below c_{min}, the waves are immediately of large amplitude and it is difficult to compute the nonlinear branch down to zero amplitude. These observations are consistent with 2D computations of Guyenne & Parau[4] and the threshold of $H_0 \approx 5$ between shallow and deep is also consistent with the fact that the *linear* depth effects are minimal for $H_0 > 5$ (see figure 1).

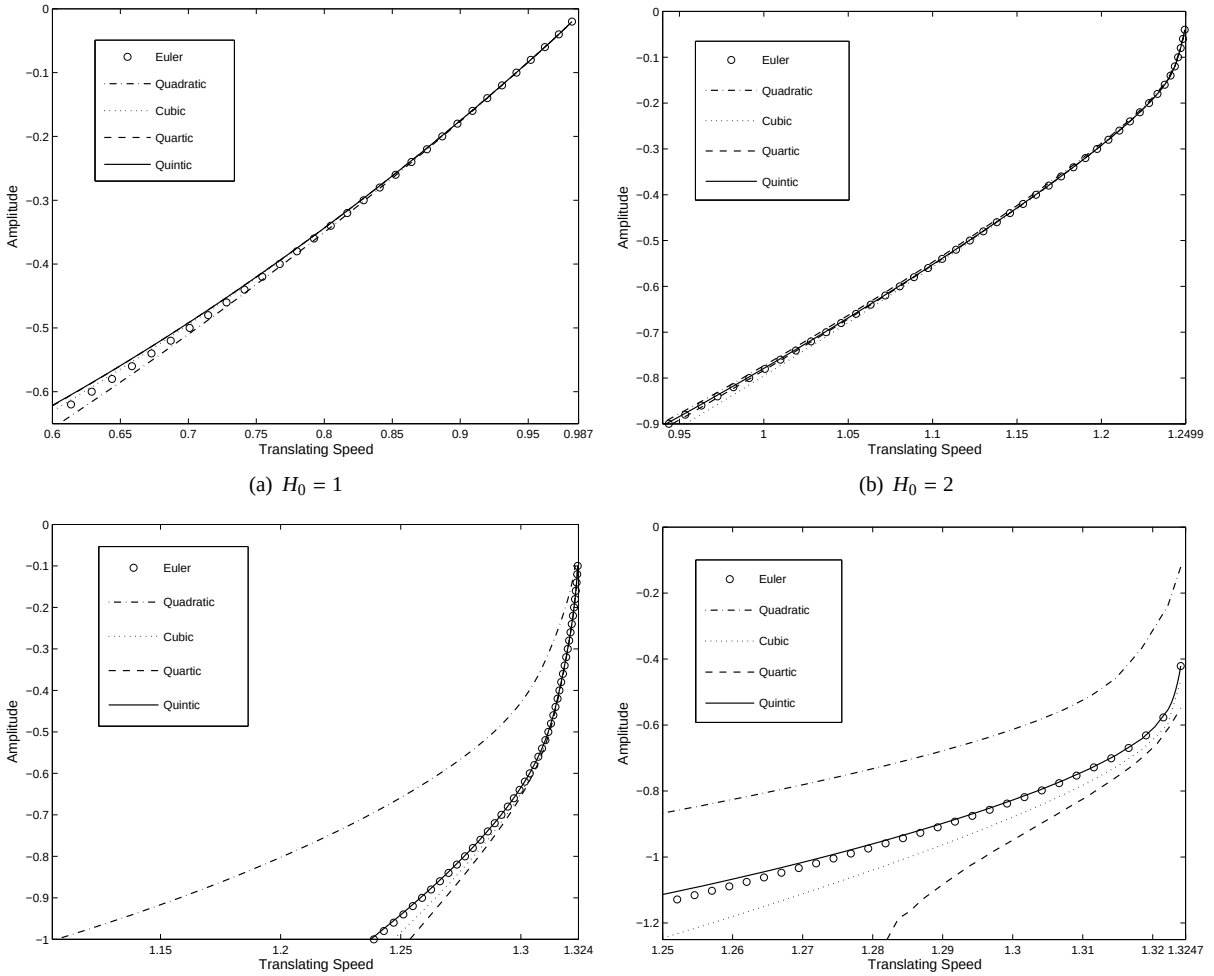

(a) $H_0 = 1$ (b) $H_0 = 2$

(c) $H_0 = 5$ (d) $H_0 = \infty$

Fig. 2. Comparison of different truncation models with the irrotational Euler system. Speed-amplitude bifurcation diagrams for 2D depression the FG solitary waves in water of different depths. Circles: full potential flow computation using a conformal mapping technique; dot-dash line: quadratic truncation model; dotted line: cubic truncation model; dashed line: quartic truncation model; solid line: quintic truncation model. (a) $H_0 = 1$, (b) $H_0 = 2$, (c) $H_0 = 5$ and (d) $H_0 = \infty$.

4.2. The Three-dimensional Problem

Focussing our attention on 3D FG solitary waves, we now seek fully localised travelling solutions for propagation speeds smaller than the minimum of the phase speed ($c < c_{min}$) and for various values of the mean depths using a fifth-order Hamiltonian truncation combined with an accurate pseudo-spectral numerical method. We write the travelling solution to the system (10–11) as

$$\eta(\theta, y) = \sum_{m=-M+1}^{M} \sum_{n=-N+1}^{N} a_{m,n} e^{i(nk\theta + mly)} \tag{19}$$

$$\xi(\theta, y) = \sum_{m=-M+1}^{M} \sum_{n=-N+1}^{N} b_{m,n} e^{i(nk\theta + mly)} \tag{20}$$

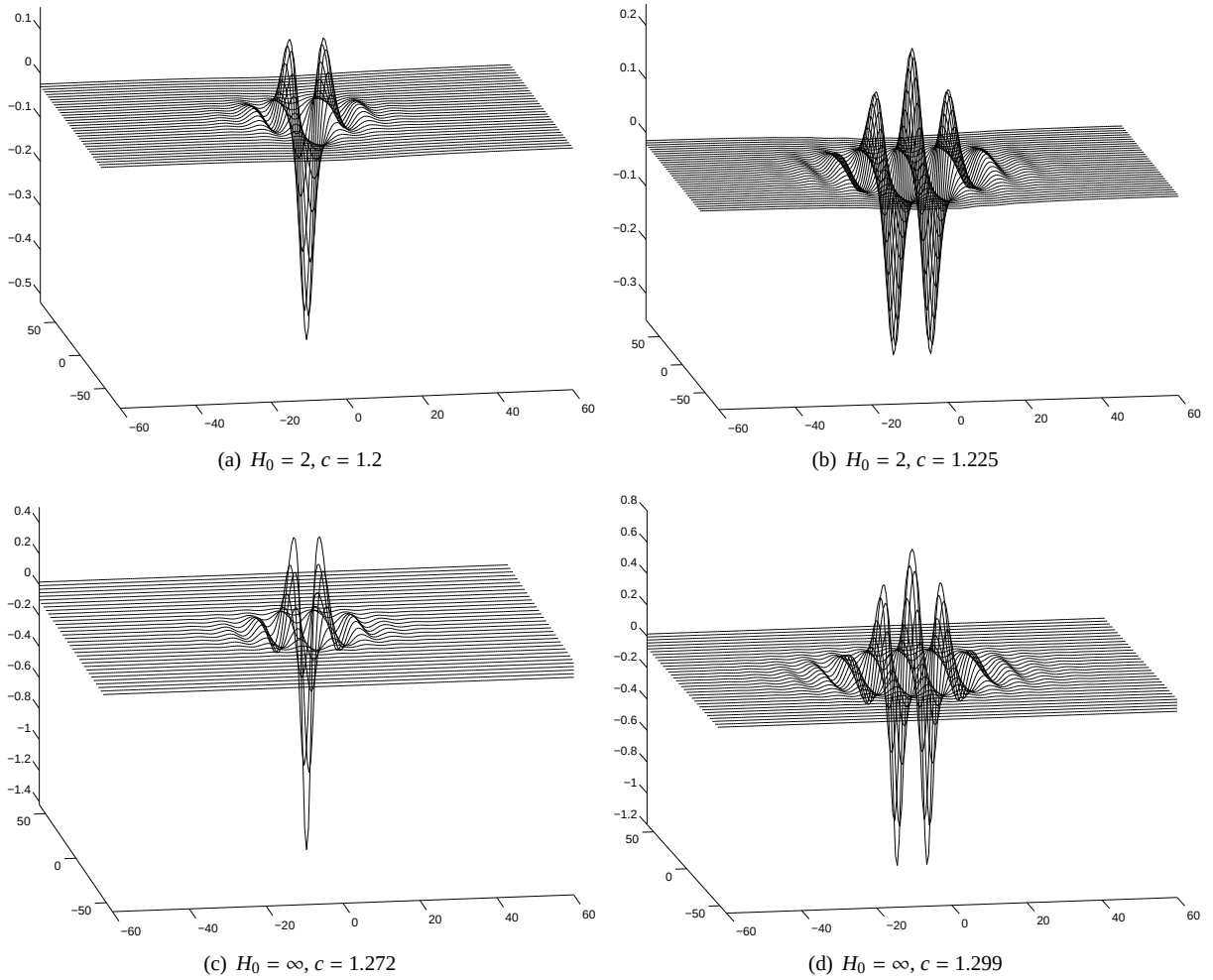

(a) $H_0 = 2$, $c = 1.2$ (b) $H_0 = 2$, $c = 1.225$

(c) $H_0 = \infty$, $c = 1.272$ (d) $H_0 = \infty$, $c = 1.299$

Fig. 3. Typical free surface profiles of depression and elevation solitary waves for the quintic model in 3D shallow and deep fluids respectively. (a) Depression wave with $\eta(0,0) = -0.5058$ and $c = 1.2$ on a fluid with the mean depth $H_0 = 2$. (b) Elevation wave with $\eta(0,0) = 0.2278$, $c = 1.225$ and $H_0 = 2$. (c) Depression wave with $\eta(0,0) = -1.4197$, $c = 1.272$ and $H_0 = \infty$. (d) Elevation wave with $\eta(0,0) = 0.7872$, $c = 1.299$ and $H_0 = \infty$. In the figures, the propagation speed c was fixed as 0.96 $c_{\min}$ for depression wave and 0.98 $c_{\min}$ for elevation wave.

with $a_{m,n} = a_{-m,n} = a_{m,-n}$ and $b_{m,n} = b_{-m,n} = -b_{m,-n}$, where $\theta = x - ct$ with the translating speed c. Both η and ξ are real and periodic on the rectangle of size $\frac{2\pi}{k}$ by $\frac{2\pi}{l}$. $a_{m,n}$ and $b_{m,n}$ are unknown Fourier coefficients which need to be solved using Newton's method, together with c. When H_0 is small, the BRDS equation is focussing and its bright soliton solution can be used to prepare the initial guess for Newton's method (see Milewski & Wang[6] for the computation of these solutions). Once such a solitary wave is found in a shallow fluid, the fully localised travelling waves in deeper fluids can be computed via straightforward continuation method using H_0 as the continuation parameter. Typical computations shown use $M = 32$ and $N = 128$.

We present in figure 3 free surface profiles of two typical cases: $H_0 = 2$ (shallower fluid, with focussing BRDS) and $H_0 = \infty$ (deep fluid, with defocussing BRDS). For each H_0 a depression solitary wave ($\eta(0,0) < 0$) and an elevation solitary wave ($\eta(0,0) > 0$) are shown at a fixed multiple of the minimal phase speed $c_{\min}(H_0)$. As expected, the waves have decaying oscillations in the direction of propagation and decay monotonically transversally to the propagation direction akin to capillary gravity waves (Wang & Milewski[15]), and corresponding to a spatially localised envelope modulating a plane wave. The principal observation from the solutions at different depths is that the shallower water

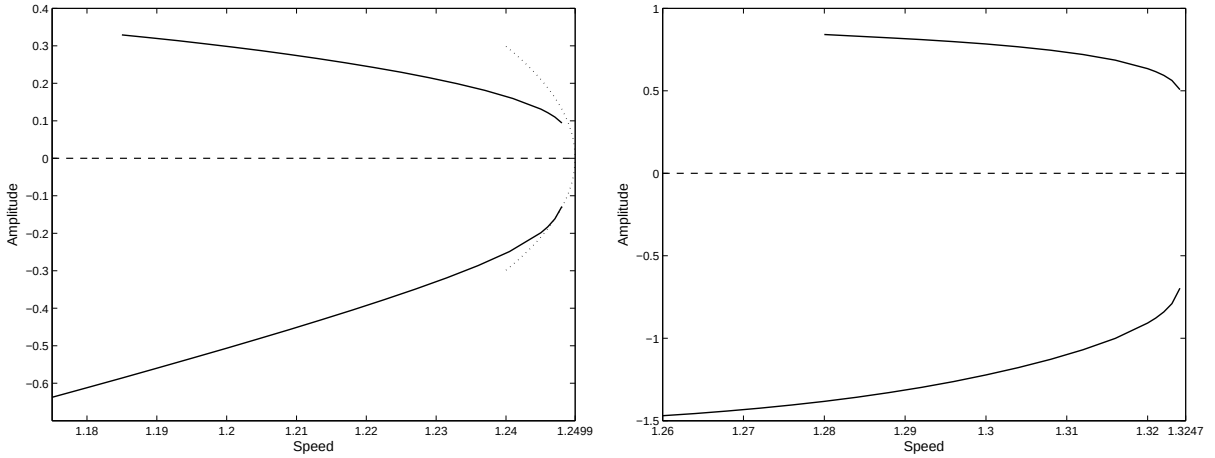

(a) $H_0 = 2$ (b) $H_0 = \infty$

Fig. 4. Speed-amplitude bifurcation diagrams. (a) $H_0 = 2$, (b) $H_0 = \infty$. The largest speed indicated on the horizontal axis is c_{min}. For the shallow water case, the asymptotic prediction is shown with a dotted line.

waves are of smaller amplitude and have longer period oscillations than deep water ones. In figure 4 we show the bifurcation curves for the two values of the depth used in figure 3. The principal observation is that for shallower water, the bifurcation curves originate from infinitesimal waves, whereas for deep water they clearly originate at finite amplitude. The shallower water bifurcation curve may thus be approximated using the solutions found in Milewski & Wang[6] and is given by

$$c - c_{min} \approx -\frac{1}{9}(\eta(0,0))^2.$$

In figure 5 we show the bifurcation diagram for $H_0 = 1$ which shows a linear relation between c and amplitude. This is an indication that a quadratically nonlinear equation of the Kadomtsev-Petviashvilli (KP) type is probably the relevant weakly nonlinear approximation in this case. Also in figure 5 are shown small and large amplitude wave profiles at $H_0 = 1$, together with a large amplitude profile for $H_0 = 2$ (the difference between this case and the small amplitude $H_0 = 2$ wave shown in figure 4 is worth noting). Both large amplitude profiles shown in figure 5 have amplitudes that are greater than half the depth of the fluid and the solution profiles are reminiscent of solitary lumps of the KP-I equation.

5. Conclusion

We have shown, using a quintic Hamiltonian model derived from the full water wave problem that three-dimensional fully localized flexural-gravity solitary waves *exist in deep water*, even though the associated Benney-Roskes-Davey-Stewartson small amplitude approximation, in this case, is of defocussing type and does not predict them. We have also computed *shallower water* localised waves, predicted by the small amplitude analysis. To our knowledge, these are the first computations of fully localised solitary flexural-gravity waves for the Plotnikov & Toland's model. The quintic model is validated by showing it is quantitatively accurate for two-dimensional flexural-gravity waves in arbitrary depth.

The Hamiltonian truncation, at any order, has its limitations. Therefore, complicated structures such as the overhanging waves found in Guyenne & Părău[3] and Wang *et al.*[16] cannot be studied using these methods and require further work. The dynamics of the waves computed here is also of interest. It is expected that small amplitude waves would be unstable (see Milewski & Wang[6]) but larger amplitude waves may be stable Wang & Milewski[15].

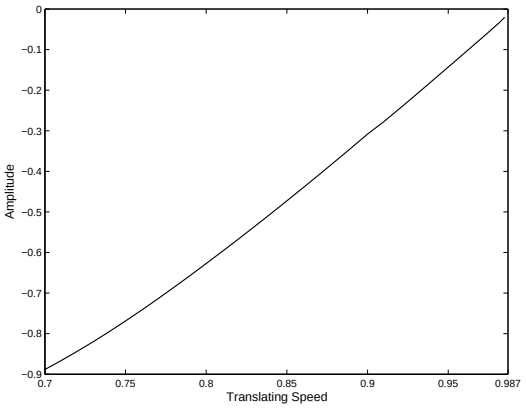

(a) $H_0 = 1$

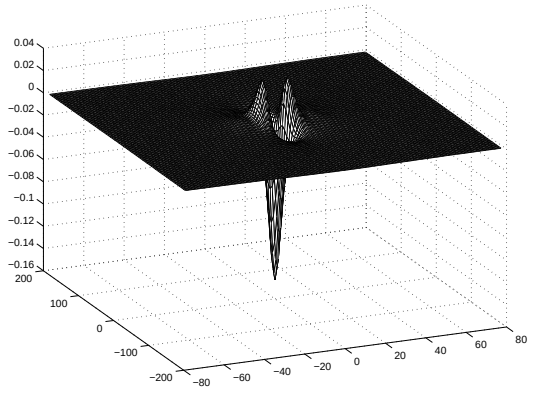

(b) $H_0 = 1$, $c = 0.95$

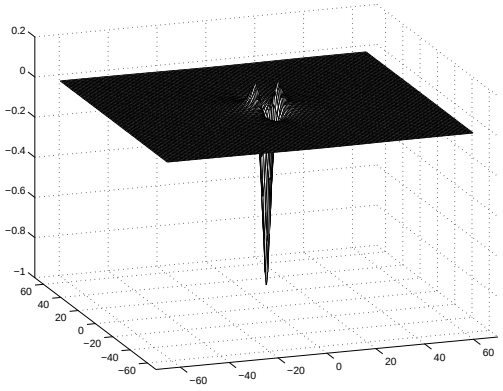

(c) $H_0 = 1$, $c = 0.7$

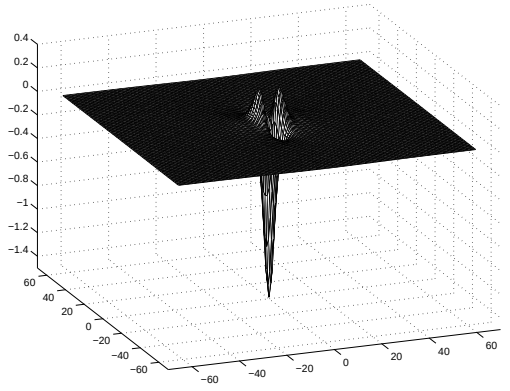

(d) $H_0 = 2$, $c = 1$

Fig. 5. (a) Depression branch for $H_0 = 1$ (b) Small amplitude depression wave $c = 0.95$ on a fluid with the mean depth $H_0 = 1$. (c) Large amplitude depression wave $c = 0.7$ on a fluid with the mean depth $H_0 = 1$. (d) Large amplitude depression wave with $c = 1$ on a fluid with the mean depth $H_0 = 2$.

Acknowledgements

This work was supported by EPSRC, under grant nos. EP/J019569/1 (J.-M.V.-B. and Z.W.) and EP/J019321/1 (P.A.M.) and by a Royal Society Wolfson award (P.A.M.).

References

1. Craig W, Nicholls DP. Traveling gravity water waves in two and three dimensions. *Euro. J. Mech. B/Fluids* 2002; **21**: 615-641.
2. Craig W, Sulem C. Numerical simulation of gravity waves. *J. Comp. Phys.* 1993; **108**: 73-83.
3. Guyenne P, Părău EI. Computations of fully nonlinear hydroelastic solitary wave on deep water. *J. Fluid Mech.* 2012; **713**: 307-329.
4. Guyenne P, Părău EI. Finite-depth effects on solitary waves in a floating ice sheet. *Submitted.*
5. Milewski PA, Vanden-Broeck JM, Wang Z. Hydroelastic solitary waves in deep water, *J. Fluid Mech.* 2011; **679**: 628-640.
6. Milewski PA, Wang Z. Three dimensional flexural-gravity waves. *Stud. Appl. Math.* 2013; doi: 10.1111/sapm.12005.
7. Nicholls DP, Reitich F. Stability of high-order methods for the computation of Dirichlet-Neumann operator. *J. Comp. Phys.* 2001; **170**: 276-298.
8. Părău EI, Dias F. Nonlinear effects in the response of a floating ice plate to a moving load. *J. Fluid Mech.* 2002; **460**: 281-305.
9. Părău EI, Vanden-Broeck JM. Three-dimensional waves beneath an ice sheet due to a steadily moving pressure. *Phil. Trans. R. Soc. A* 2011; **369**: 2973-2988.

10. Părău EI, Vanden-Broeck JM. Three-dimensional nonlinear waves under an ice sheet and related flows. In Proc. of the 21th Int. Offshore and Polar Eng. Conf. (ISOPE), Maui, Hawaii, 19-24 June 2011. Mountain View, CA: ISOPE.
11. Părău EI, Vanden-Broeck JM, Cooker MJ. Nonlinear three-dimensional gravity-capillary solitary waves. *J. Fluid Mech.* 2005; **536**: 99-105.
12. Plotnikov PI, Toland JF. Modelling nonlinear hydroelastic waves. *Phil. Trans. R. Soc. Lond. A* 2011; **369**: 2942-2956.
13. Squire VA, Hosking RJ, Kerr AD, Langhorne PJ. *Moving Loads on Ice Plates. (Solid Mechanics and Its Applications)*. Kluwer; 1999.
14. Sulem C, Sulem PL. *The nonlinear Schrödinger equation: self-focusing and wave collapse*. Applied Mathematical Sciences, Vol. 139, Springer-Verlag, New York; 1999.
15. Wang Z, Milewski PA. Dynamics of gravity-capillary solitary waves in deep water. *J. Fluid Mech.* 2012; **708**: 480-501.
16. Wang Z, Vanden-Broeck JM, Milewski PA. Two-dimensional flexural-gravity waves of finite amplitude in deep water. *IMA J. Appl. Math.* 2013; doi:10.1093/imamat/hxt020.
17. Xu L, Guyenne P. Numerical simulation of three-dimensional nonlinear water waves. *J. Comp. Phys.* 2009; **228**: 8446-8466.
18. Zakharov VE. Stability of periodic waves of finite amplitude on the surface of a deep fluid. *J. Appl. Mech. Tech. Phys.* 1968; **2**: 190-194.